HHS Public Access

Author manuscript

Genesis. Author manuscript; available in PMC 2019 June 28.

Published in final edited form as:

Genesis. 2018 June ; 56(6-7): e23214. doi:10.1002/dvg.23214.

Tracking neural crest cell cycle progression *in vivo*

Sriivatsan G. Rajan[1,†], **Kristin L. Gallik**[1,†], **James R. Monaghan**[2], **Rosa A. Uribe**[3], **Marianne E. Bronner**[4], and **Ankur Saxena**[1]

[1]Department of Biological Sciences, University of Illinois at Chicago, Chicago, IL 60607, USA

[2]Department of Biology, Northeastern University, Boston, MA 02131, USA

[3]Department of Biosciences, Rice University, Houston TX, 77005

[4]Division of Biology and Biological Engineering, California Institute of Technology, Pasadena, CA 91125, USA

Abstract

Analysis of cell cycle entry/exit and progression can provide fundamental insights into stem cell propagation, maintenance, and differentiation. The neural crest is a unique stem cell population in vertebrate embryos that undergoes long-distance collective migration and differentiation into a wide variety of derivatives. Using traditional techniques such as immunohistochemistry to track cell cycle changes in such a dynamic population is challenging, as static time points provide an incomplete spatiotemporal picture. By contrast, the fluorescent, ubiquitination-based cell cycle indicator (Fucci) system provides *in vivo* readouts of cell cycle progression and has been previously adapted for use in zebrafish. The most commonly used Fucci systems are ubiquitously expressed, making tracking of a specific cell population challenging. Therefore, we generated a transgenic zebrafish line, *Tg(−4.9sox10:mAG-gmnn(1/100)-2A-mCherry-cdt1(1/190))*, in which the Fucci system is specifically expressed in delaminating and migrating neural crest cells. Here, we demonstrate validation of this new tool and its use in live high-resolution tracking of cell cycle progression in the neural crest and derivative populations.

Keywords

zebrafish; Fucci; Sox10

1 INTRODUCTION

The neural crest is a unique population of highly migratory stem cells that contributes to the development and formation of multiple tissues in vertebrates (Bronner & LeDouarin, 2012; Gallik et al., 2017). Migrating neural crest cells (NCCs) progress through the cell cycle with variable timing, rates, and frequency, the details of which are likely critical for the initiation of migration and maintenance of migratory stream dynamics (Burstyn-Cohen and Kalcheim,

Correspondence: Ankur Saxena, Department of Biological Sciences, University of Illinois at Chicago, Chicago, IL 60607, USA. saxenaa@uic.edu.

[†]These authors contributed equally to this work.

The authors have no conflicts of interest to declare.

2002; Ridenour et al., 2014). Some of the most commonly used techniques to monitor NCC proliferation include immunostaining for pH3 or Ki-67 and incorporation of BrdU or EdU, all analyzed in fixed tissue samples (Gonsalvez et al., 2015; Ridenour et al., 2014). While these techniques can reveal many important aspects of cell cycle progression, they only allow for 'snapshots' of information. A cell population as dynamic, diverse, and migratory as the neural crest can benefit from a live readout of cell cycle dynamics over the course of delamination, migration, and differentiation.

The fluorescent, ubiquitination-based cell cycle indicator (Fucci) system was originally developed in human cell culture and mice to provide live readouts of G1 to S phase transition in actively dividing cells (Sakaue-Sawano et al., 2008). This innovative system uses chimeric proteins made of fluorophores fused to truncated forms of Cdt1 (marking G1 phase) and Geminin (marking S/G2/M phases) that are targeted for ubiquitin tagging and degradation during cell cycle progression. Fucci has been previously adapted for use in zebrafish via two ubiquitously expressed transgenic constructs that separately express the chimeric proteins monomeric Azami Green (mAG)-zGem(1/100) and monomeric Kusabira Orange2-zCdt1(1/190) (Sugiyama et al., 2009). In order to remove the need for maintaining separate transgenic constructs in the same animal, the zebrafish Fucci system was more recently augmented to express Cerulean-zGem(1/100) and mCherry-zCdt1(1/190) from the same ubiquitous promoter (Bouldin & Kimelman, 2014). While ubiquitous Fucci systems are highly proficient at revealing global changes in cell cycle progression during vertebrate development, additional cell-specific markers are required to track a cell population such as the neural crest. This task is further complicated by the challenges of (1) separating out densely packed, ubiquitously labeled cells; (2) cell tracking and lineage tracing of a highly migratory population; (3) dedication of multiple channels to imaging the Fucci system. To alleviate these complications, we generated a zebrafish Fucci system to track cell cycle progression specifically in NCCs and their derivatives during embryonic development.

We used the previously described −4.9 kb promoter/enhancer region for Sox10 (Wada et al., 2005), a transcription factor expressed specifically in NCCs at early developmental stages (Dutton et al., 2001), to drive the expression of a bicistronic construct of the fusion proteins mAG-zGem(1/100) and mCherry-zCdt1(1/190). We used this construct to create a stable transgenic zebrafish line, *Tg(−4.9sox10:mAG-gmnn(1/100)-2A-mCherry-cdt1(1/190)),* here referred to for simplicity as Sox10:zFucci. We validated accurate marking of the cell cycle using immunofluorescence staining against pH3, a marker for G2/M phases (Hendzel et al., 1997). Additionally, we compared the expression pattern of Sox10:zFucci to the Sox10:mRFP transgenic line (*Tg(−7.2sox10:mRFP)*; Kucenas, Snell, & Appel, 2008) and the Sox10:eGFP transgenic line (*Tg(−4.9sox10:eGFP)*; Wada et al., 2005) at several stages of development. Our data establish that Sox10:zFucci accurately follows cell cycle progression in NCCs early in development and subsequently in other cell types, including in NCC derivatives.

2 RESULTS AND DISCUSSION

In Sox10:zFucci zebrafish, the −4.9 kb Sox10 promoter/enhancer drives a bicistronic construct containing the fusion proteins mAG-zGem(1/100) and mCherry-zCdt1(1/190)

separated by a viral 2A peptide (Figure 1a). For clarity, cells expressing green nuclear mAG-zGem(1/100) will be referred to here as Sox10:zFucci (S/G2/M), and cells expressing red nuclear mCherry-zCdt1(1/190) will be referred to as Sox10:zFucci (G1).

To determine if Sox10:zFucci is neural crest-specific while NCCs are delaminating and migrating, we crossed the Sox10:zFucci line with the Sox10:mRFP line, which is commonly used to label NCCs (Blasky, Pan, Moens, & Appel, 2014; Leigh et al., 2013). We performed time-lapse confocal microscopy of Sox10:zFucci; Sox10:mRFP-dual positive embryos from 14 to 23 hours post-fertilization (hpf) or 13 to 28 hpf (Figure 1b–e; Movies 1–2). At 14 hpf, nearly all Sox10:zFucci-positive cells were positive for Sox10:mRFP (Figure 1b). Within the same embryos, we followed a subset of Sox10:zFucci-positive cells that were not initially Sox10:mRFP-postive and found that they expressed Sox10:mRFP by 15 hpf (Figure 1b,c; insets). Additionally, by 16 hpf, some Sox10:mRFP-positive cells were no longer Sox10:zFucci-positive (Figure 1d). Throughout the time-lapses, Sox10:zFucci; Sox10:mRFP-dual positive cells were seen migrating ventrolaterally, contributing to a continual decrease in the number of Sox10:zFucci-positive cells on the anterodorsal side of the developing embryo. Additionally, a few Sox10:zFucci; Sox10:mRFP-dual positive cells were seen transitioning from G1 to S phase as indicated by red nuclei turning yellow and then green (Figure 1b, arrowheads; e), providing a useful tool for tracking NCCs progressing through the G1/S checkpoint *in vivo*. To verify the dynamics of our cell cycle indicators, we tracked Sox10:zFucci-positive cells transitioning through cell division every 10’ (Movie 2; Figure 1e shows a subset of data every 20’) and quantified the mAG-zGem(1/100) and mCherry-zCdt1(1/190) fluorescence levels (Figure 1f) of the cell shown in Figure 1e. We observed an inverse correlation in fluorescence intensity of the two indicators before and during cell division (Figure 1f)that was consistent with previously reported zFucci dynamics (Sugiyama et al., 2009). These data indicate that Sox10:zFucci expression is regulated by ubiquitin-mediated degradation of mAG-zGem(1/100) and mCherry-zCdt1(1/190) at appropriate stages of the cell cycle. Importantly, all observed Sox10:zFucci-positive cells were eventually positive for Sox10:mRFP. Collectively, these observations indicate that Sox10:zFucci expression is neural crest-specific at early stages of development and regulated appropriately throughout the cell cycle.

To further verify that Sox10:zFucci accurately distinguishes between dividing and non-dividing NCCs, we performed whole-mount immunohistochemistry against pH3 to detect cells that were in G2 or M phase (Hendzel et al., 1997) at 13, 17, 21, and 25 hpf in Sox10:zFucci-positive embryos (Figure 2). Previous studies in zebrafish have shown that at 13 hpf, many NCCs are delaminating from the dorsal neuroepithelium, and at 17 hpf, large numbers of NCCs are migrating (Berndt, Clay, Langenberg, & Halloran, 2008; Jimenez et al., 2016). Therefore, we focused on the anterodorsal side of the embryo at 13 and 17 hpf and followed up with subsequent time points at 21 and 25 hpf to validate the continued expression of Sox10:zFucci in migrating NCCs. At 13 hpf, only 0.69 ± 0.39% of observed Sox10:zFucci (S/G2/M)-positive cells were positive for G2/M-specific pH3 (n = 680 Sox10:zFucci (S/G2/M)-positive cells across 3 embryos; Figures 2a,a’; S1), suggesting that a large number of NCCs are in the S phase at this time point. These data are consistent with previous work in chicken embryos suggesting that many NCCs begin migrating while in S phase (Burstyn-Cohen & Kalcheim, 2002). Four hours later, at 17 hpf, 9.84 ± 1.46% of

observed Sox10:zFucci (S/G2/M)-positive cells were positive for pH3 (n = 347 Sox10:zFucci (S/G2/M)-positive cells across 3 embryos; Figure 2b,b'; S1). At 21 hpf, 3.98 ± 1.71% of observed Sox10:zFucci (S/G2/M)-positive cells were pH3-positive (n = 165 Sox10:zFucci (S/G2/M)-positive cells across 3 embryos; Figure 2c,c'; S1). At 25 hpf, none of the observed Sox10:zFucci (S/G2/M)-positive cells were positive for pH3 (n = 44 Sox10:zFucci (S/G2/M)-positive cells across 3 embryos; Figure 2d,d'; S1). Importantly, at all observed time points, none of the observed Sox10:zFucci (G1)-positive cells were positive for pH3 (n = 1335 Sox10:zFucci (G1)-positive cells across 12 embryos; Figure 2a",b",c",d"). Cumulatively, these data suggest that Sox10:zFucci acts as a reliable indicator of cell cycle progression at multiple stages of development.

NCCs contribute to a wide variety of cell types in both the craniofacial and trunk regions of the developing embryo that often continue to express Sox10-driven transgenic lines (Carney et al., 2006; Rochard, Ling, Kong, & Liao, 2015; Saxena, Peng, & Bronner, 2013; Schweizer, Ayer-Le Lievre, & Le Douarin, 1983; Wada et al., 2005). To determine if Sox10:zFucci is similarly expressed in neural crest-derived craniofacial derivatives, we crossed the Sox10:zFucci line with the Sox10:eGFP line, imaged Sox10:zFucci; Sox10:eGFP-dual positive embryos, and used the image processing software Imaris (Bitplane, Inc.) to map out all cells expressing Sox10:zFucci (G1) and/or Sox10:eGFP. At 37 hpf, 89.07 ± 1.72% of Sox10:eGFP-positive microvillous neurons in the olfactory epithelium were Sox10:zFucci (G1)-positive (n = 395 Sox10:eGFP-positive cells across 6 embryos; Figure 3a–b"'; S2). At 96 hpf, 65.51 ± 2.07% of observed Sox10:eGFP-positive cartilage cells in the jaw were also Sox10:zFucci (G1)-positive (n = 4572 Sox10:eGFP-positive cells across 6 embryos; Figure 3c–d"'; S2). In the trunk, we focused on the dorsal root ganglia (DRG), where 86.46 ± 3.31% of observed Sox10:eGFP-positive DRG neurons were Sox10:zFucci (G1)-positive at 37 hpf (n = 214 Sox10:eGFP-positive cells across 6 embryos; Figure 3e–f"'; S2). Collectively, our results suggest that the majority of Sox10:eGFP-positive microvillous neurons and DRG neurons are dual positive for Sox10:zFucci (G1) (Figure S2), consistent with the known expression of zCdt1(1/190) in differentiated post-mitotic neurons (Sugiyama et al., 2009). The lower percentage (65.51%) of Sox10:zFucci (G1)-positive cells in the craniofacial cartilage (Figure S2) is consistent with previous studies that have shown the zebrafish craniofacial cartilage at 96 hpf to consist of a mixture of proliferating, growing, and differentiating chondrocytes (Rochard, Ling, Kong, & Liao, 2015). Additionally, Sox10:zFucci marked neural crest-derived Sox10:eGFP-positive melanocytes (Figure S3). Taken together, our data indicate that Sox10:zFucci successfully marks multiple neural crest-derived populations of Sox10:eGFP-positive cells at several stages of embryogenesis.

While Sox10 is a robust marker for many neural crest lineages, Sox10-driven lines also label some other non-neural crest-derived cell populations at later time points. For example, multiple studies have used Sox10:eGFP and Sox10:mRFP to mark oligodendrocytes (Chung, Kim, Kim, Bae, & Park, 2011; Kucenas, Snell, & Appel, 2008) and otic epithelial cells (Carney et al., 2006; Kwak et al., 2013). To determine if Sox10:zFucci is also expressed in these cell types, we crossed the Sox10:zFucci line with either the Sox10:mRFP or Sox10:eGFP line. At 24 hpf, a subset of cells marked by Sox10:mRFP in the otic epithelium was Sox10:zFucci (S/G2/M)-positive (Figure 4a–a"). At both 36 hpf and 57 hpf,

oligodendrocyte progenitor cells in the hindbrain marked by Sox10:eGFP were Sox10:zFucci-positive (Figure 4b–c”). Sox10:eGFP-positive muscle cells (Rodrigues, Doughton, Yang, & Kelsh, 2012) were also Sox10:zFucci-positive (Figure 4b–b”). These data from multiple cell types show that Sox10:zFucci successfully labels some Sox10-expressing non-neural crest-derived cell types.

In summary, we have created a new cell type-specific Fucci system, Sox10:zFucci, to track cell cycle progression at high spatiotemporal resolution in NCCs and other cell types during embryonic development. Sox10:zFucci faithfully indicates phases of the cell cycle and is expressed specifically in delaminating and migrating NCCs during early- to mid-somitogenesis. Later in development, Sox10:zFucci recapitulates the expression of Sox10:eGFP and Sox10:mRFP in both neural crest-derived and non-neural crest-derived tissues. Studies of signaling pathways that alter the cell cycle in NCCs or particular derivatives will benefit from Sox10:zFucci’s live readout of cell cycle entry/exit and progression *in vivo*.

3 MATERIALS & METHODS

3.1 Zebrafish

Animals were treated and cared for in accordance with the National Institutes of Health Guide for the Care and Use of Laboratory animals. All experiments were approved by the University of Illinois at Chicago Institutional Animal Care and Use Committee (IACUC). Embryos were grown, staged, and harvested as previously described (Kimmel, Ballard, Kimmel, Ullmann, & Schilling, 1995; Westerfield, 2000). All embryos to be used at time points older than 24 hours post-fertilization (hpf) were treated with 1-phenyl-2-thiourea (PTU) to prevent pigmentation from interfering with imaging. Transgenic lines used and their abbreviations here are: *Tg(−4.9sox10:eGFP)* (Wada et al., 2005) = Sox10:eGFP; *Tg(−7.2sox10:mRFP)* (Kucenas et al., 2008) = Sox10:mRFP; *Tg(−4.9sox10:mAG-gmnn(1/100)-2A-mCherry-cdt1(1/190))* = Sox10:zFucci.

3.2 Generation of Sox10:zFucci

Using the Gateway cloning system via LR Clonase II Plus enzyme (Invitrogen), mAG-zGem(1/100) was cloned upstream of mCherry-zCdt1(1/190), separated by the viral T2A peptide, and placed downstream of the −4.9kb Sox10 promoter in a plasmid containing Tol2 elements, creating *−4.9sox10:mAG-gmnn(1/100)-2A-mCherry-cdt1(1/190)*. The following entry and destination vector plasmids were used: p5E-sox10 (Uribe, Hong, & Bronner, 2018), pME-mAG-zGem(1/100) (Sugiyama *et al.*, 2009), p3E-T2A-mCherry-zCdt1(1/190)pA and pDest-Tol2pA2 (Kwan et al., 2007). One-cell stage embryos were injected with *pDEST-4.9sox10:mAG-gmnn(1/100)-2A-mCherry-cdt1(1/190)pA2* to generate a stable line as previously described (Kawakami, Shima, & Kawakami, 2000). The Sox10:zFucci line does not appear to cause any phenotypes in heterozygous and homozygous embryos. The line will be made freely available to the research community upon request.

3.3 Live Confocal Imaging

Embryos were prepared for imaging as previously described (Kaufmann, Mickoleit, Weber, & Huisken, 2012; Saxena & Bronner, 2014). Confocal time-lapse microscopy was performed on a Zeiss LSM 800 microscope with a 40×/1.1 W objective. Collected data were processed and analyzed using Imaris (Bitplane, Inc.) and exported as TIFF images or AVI movies. The Imaris 'Spots Analysis' feature was used to track individual NCCs progressing through the cell cycle in Sox10:zFucci; Sox10:mRFP-dual positive embryos and measure Sox10:zFucci fluorescence intensity throughout the cell cycle. The 'Colocalize Spots' extension for Imaris was used to analyze confocal z-stacks for colocalization of Sox10:zFucci (G1) and Sox10:eGFP.

3.4 Immunofluorescence Staining

Sox10:zFucci-positive embryos were collected at 13, 17, 21, and 25 hpf, fixed with 4% PFA, and washed in PBS. Some embryos were incubated in acetone at −20°C for 20'. Embryos were then washed in PBDT (1% BSA, 1% DMSO, 0.1% Triton X-100 in PBS, pH 7.4), blocked in 10% normal donkey serum/PBDT, and incubated overnight at 4°C with MsαpH3 (1:500; Abcam ab14955). Further PBDT washes and blocking were followed by overnight incubation at 4°C with Alexa Fluor DkαMs647 (1:1000; ThermoFisher A-31571) and Hoechst 34580 (1:2500). Secondary antibody incubation was followed with additional PBDT, PBST, and PBS washes. Embryos were prepared for confocal imaging as previously described (Saxena & Bronner, 2014). Both Sox10:zFucci fluorophores, Azami Green and mCherry, continued to fluoresce brightly after completion of our immunofluorescence protocol and were imaged directly. Confocal microscopy was performed on a Zeiss LSM 800 microscope with a 40×/1.1 W objective. The 'Colocalize Spots' extension for Imaris was used to analyze confocal z-stacks for colocalization of pH3 with mAG-zGem(1/100) or mCherry-zCdt1(1/190). Data were exported as TIFF images.

Supplementary Material

Refer to Web version on PubMed Central for supplementary material.

Acknowledgments

The authors would like to thank Daniel Koshy and Fritz Gerald D. Navales for imaging assistance; Randall W. Treffy for feedback and guidance on the manuscript; Dr. Robert Kelsh for the Sox10:eGFP line; Dr. Bruce Appel for the Sox10:mRFP line. This work was funded by the Chicago Biomedical Consortium with support from the Searle Funds at The Chicago Community Trust (#C-070) to A.S., NIH NRSA HD080343 to R.A.U., and NIH R01-DE024157 to M.E.B.

References

Berndt JD, Clay MR, Langenberg T, Halloran MC. Rho-kinase and myosin II affect dynamic neural crest cell behaviors during epithelial to mesenchymal transition in vivo. Dev Biol. 2008; 324(2): 236–244. DOI: 10.1016/j.ydbio.2008.09.013 [PubMed: 18926812]

Blasky AJ, Pan L, Moens CB, Appel B. Pard3 regulates contact between neural crest cells and the timing of Schwann cell differentiation but is not essential for neural crest migration or myelination. Dev Dyn. 2014; 243(12):1511–1523. DOI: 10.1002/dvdy.24172 [PubMed: 25130183]

Bouldin CM, Kimelman D. Cdc25 and the importance of G2 control: insights from developmental biology. Cell Cycle. 2014; 13(14):2165–2171. DOI: 10.4161/cc.29537 [PubMed: 24914680]

Bronner ME, LeDouarin NM. Development and evolution of the neural crest: an overview. Dev Biol. 2012; 366(1):2–9. DOI: 10.1016/j.ydbio.2011.12.042 [PubMed: 22230617]

Burstyn-Cohen T, Kalcheim C. Association between the cell cycle and neural crest delamination through specific regulation of G1/S transition. Dev Cell. 2002; 3(3):383–395. DOI: 10.1016/S1534-5807(02)00221-6 [PubMed: 12361601]

Carney TJ, Dutton KA, Greenhill E, Delfino-Machin M, Dufourcq P, Blader P, Kelsh RN. A direct role for Sox10 in specification of neural crest-derived sensory neurons. Development. 2006; 133(23):4619–4630. DOI: 10.1242/dev.02668 [PubMed: 17065232]

Chung AY, Kim S, Kim H, Bae YK, Park HC. Microarray screening for genes involved in oligodendrocyte differentiation in the zebrafish CNS. Exp Neurobiol. 2011; 20(2):85–91. DOI: 10.5607/en.2011.20.2.85 [PubMed: 22110365]

Dutton KA, Pauliny A, Lopes SS, Elworthy S, Carney TJ, Rauch J, Kelsh RN. Zebrafish colourless encodes sox10 and specifies non-ectomesenchymal neural crest fates. Development. 2001; 128(21):4113–4125. [PubMed: 11684650]

Gallik KL, Treffy RW, Nacke LM, Ahsan K, Rocha M, Green-Saxena A, Saxena A. Neural crest and cancer: Divergent travelers on similar paths. Mech Dev. 2017; 148:89–99. DOI: 10.1016/j.mod.2017.08.002 [PubMed: 28888421]

Gonsalvez DG, Li-Yuen-Fong M, Cane KN, Stamp LA, Young HM, Anderson CR. Different neural crest populations exhibit diverse proliferative behaviors. Dev Neurobiol. 2015; 75(3):287–301. DOI: 10.1002/dneu.22229 [PubMed: 25205394]

Hendzel MJ, Wei Y, Mancini MA, Van Hooser A, Ranalli T, Brinkley BR, Allis CD. Mitosis-specific phosphorylation of histone H3 initiates primarily within pericentromeric heterochromatin during G2 and spreads in an ordered fashion coincident with mitotic chromosome condensation. Chromosoma. 1997; 106(6):348–360. DOI: 10.1007/s004120050256 [PubMed: 9362543]

Jimenez L, Wang J, Morrison MA, Whatcott C, Soh KK, Warner S, Stewart RA. Phenotypic chemical screening using a zebrafish neural crest EMT reporter identifies retinoic acid as an inhibitor of epithelial morphogenesis. Dis Model Mech. 2016; 9(4):389–400. DOI: 10.1242/dmm.021790 [PubMed: 26794130]

Kaufmann A, Mickoleit M, Weber M, Huisken J. Multilayer mounting enables long-term imaging of zebrafish development in a light sheet microscope. Development. 2012; 139(17):3242–3247. DOI: 10.1242/dev.082586 [PubMed: 22872089]

Kawakami K, Shima A, Kawakami N. Identification of a functional transposase of the Tol2 element, an Ac-like element from the Japanese medaka fish, and its transposition in the zebrafish germ lineage. Proc. Natl. Acad. Sci. U.S.A. 2000; 97(21):11403–11408. DOI: 10.1073/pnas.97.21.11403 [PubMed: 11027340]

Kimmel CB, Ballard WW, Kimmel SR, Ullmann B, Schilling TF. Stages of embryonic development of the zebrafish. Dev Dyn. 1995; 203(3):253–310. DOI: 10.1002/aja.1002030302 [PubMed: 8589427]

Kucenas S, Snell H, Appel B. nkx2.2a promotes specification and differentiation of a myelinating subset of oligodendrocyte lineage cells in zebrafish. Neuron Glia Biol. 2008; 4(2):71–81. DOI: 10.1017/S1740925X09990123 [PubMed: 19737431]

Kwak J, Park OK, Jung YJ, Hwang BJ, Kwon SH, Kee Y. Live image profiling of neural crest lineages in zebrafish transgenic lines. Mol Cells. 2013; 35(3):255–260. DOI: 10.1007/s10059-013-0001-5 [PubMed: 23456294]

Kwan KM, Fujimoto E, Grabher C, Mangum BD, Hardy ME, Campbell DS, Chien CB. The Tol2kit: a multisite gateway-based construction kit for Tol2 transposon transgenesis constructs. Dev Dyn. 2007; 236(11):3088–3099. DOI: 10.1002/dvdy.21343 [PubMed: 17937395]

Leigh NR, Schupp MO, Li K, Padmanabhan V, Gastonguay A, Wang L, Ramchandran R. Mmp17b is essential for proper neural crest cell migration in vivo. PLoS One. 2013; 8(10):e76484.doi: 10.1371/journal.pone.0076484 [PubMed: 24098510]

Ridenour DA, McLennan R, Teddy JM, Semerad CL, Haug JS, Kulesa PM. The neural crest cell cycle is related to phases of migration in the head. Development. 2014; 141(5):1095–1103. DOI: 10.1242/dev.098855 [PubMed: 24550117]

Rochard LJ, Ling IT, Kong Y, Liao EC. Visualization of Chondrocyte Intercalation and Directional Proliferation via Zebrabow Clonal Cell Analysis in the Embryonic Meckel's Cartilage. J Vis Exp. 2015; (105):e52935.doi: 10.3791/52935 [PubMed: 26555721]

Rodrigues FS, Doughton G, Yang B, Kelsh RN. A novel transgenic line using the Cre-lox system to allow permanent lineage-labeling of the zebrafish neural crest. Genesis. 2012; 50(10):750–757. DOI: 10.1002/dvg.22033 [PubMed: 22522888]

Sakaue-Sawano A, Kurokawa H, Morimura T, Hanyu A, Hama H, Osawa H, Miyawaki A. Visualizing spatiotemporal dynamics of multicellular cell-cycle progression. Cell. 2008; 132(3):487–498. DOI: 10.1016/j.cell.2007.12.033 [PubMed: 18267078]

Saxena A, Bronner ME. A novel HoxB cluster protein expressed in the hindbrain and pharyngeal arches. Genesis. 2014; 52(10):858–863. DOI: 10.1002/dvg.22806 [PubMed: 25137177]

Saxena A, Peng BN, Bronner ME. Sox10-dependent neural crest origin of olfactory microvillous neurons in zebrafish. eLife. 2013; 2:e00336.doi: 10.7554/eLife.00336 [PubMed: 23539289]

Schweizer G, Ayer-Le Lievre C, Le Douarin NM. Restrictions of developmental capacities in the dorsal root ganglia during the course of development. Cell Differ. 1983; 13(3):191–200. DOI: 10.1016/0045-6039(83)90089-1 [PubMed: 6667495]

Sugiyama M, Sakaue-Sawano A, Iimura T, Fukami K, Kitaguchi T, Kawakami K, Miyawaki A. Illuminating cell-cycle progression in the developing zebrafish embryo. Proc Natl Acad Sci U S A. 2009; 106(49):20812–20817. DOI: 10.1073/pnas.0906464106 [PubMed: 19923430]

Uribe RA, Hong SS, Bronner ME. Retinoic acid temporally orchestrates colonization of the gut by vagal neural crest cells. Dev Biol. 2018; 433(1):17–32. DOI: 10.1016/j.ydbio.2017.10.021 [PubMed: 29108781]

Wada N, Javidan Y, Nelson S, Carney TJ, Kelsh RN, Schilling TF. Hedgehog signaling is required for cranial neural crest morphogenesis and chondrogenesis at the midline in the zebrafish skull. Development. 2005; 132(17):3977–3988. DOI: 10.1242/dev.01943 [PubMed: 16049113]

Westerfield M. The zebrafish book. A guide for the laboratory use of zebrafish (Danio rerio). 4. Eugene: University of Oregon Press; 2000.

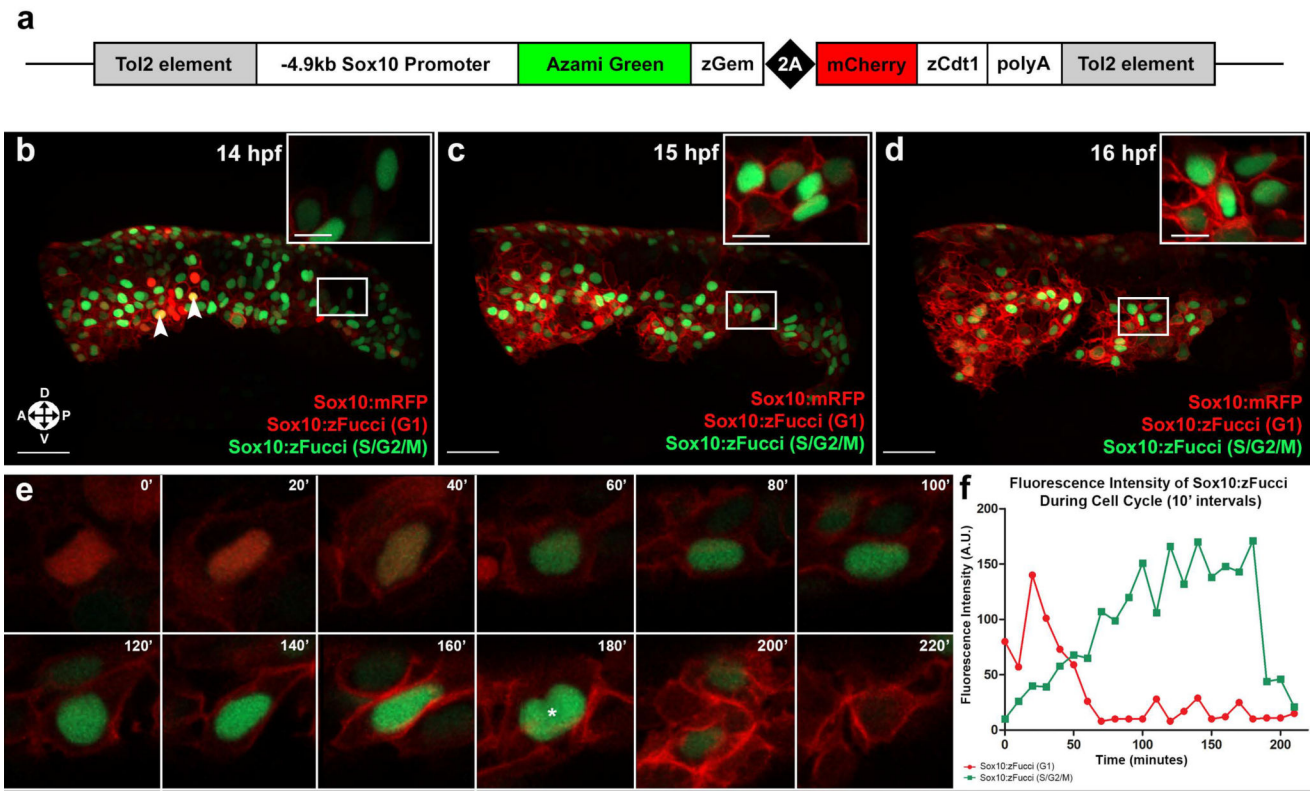

Figure 1. Overlap of Sox10:zFucci and Sox10:mRFP expression in delaminating and migrating neural crest cells

(a) Schematic of the *Tg(−4.9sox10:mAG-gmnn(1/100)-2A-mCherry-cdt1(1/190))* (Sox10:zFucci) transgenic construct. (b–d) 3D projections of lateral views of a representative Sox10:zFucci; Sox10:mRFP-dual positive embryo at 14 (b), 15 (c), and 16 (d) hours post-fertilization (hpf). Insets (b,c,d) show optical slices (4.5 μm thick) of a subset of Sox10:zFucci-positive cells that become Sox10:mRFP-positive as the embryo develops. Arrowheads (b) indicate Sox10:zFucci (G1); Sox10:zFucci (S/G2/M)-dual positive cells. (e) Optical slices (4.4 μm thick) of a single Sox10:zFucci; Sox10:mRFP-dual positive neural crest cell from Movie 2 (10' interval time-lapse) transitioning through the cell cycle (panels shown every 20'). At 40', the cell is seen transitioning from G1 to S phase as indicated by a yellow nucleus and is then seen dividing at 180' (asterisk). After division (200'), zFucci fluorescence quickly diminishes in daughter cells by 220'. (f) Fluorescence intensities (arbitrary units: A.U.) of Sox10:zFucci (G1) and Sox10:zFucci (S/G2/M) every 10' over a period of 220' in the cell shown in (e). Sox10:mRFP: red membranes; Sox10:zFucci (G1): red nuclei; Sox10:zFucci (S/G2/M): green nuclei. Orientation arrows: A: anterior; P: posterior; D: dorsal; V: ventral. Scale bars: 50 μm; insets: 12.5 μm.

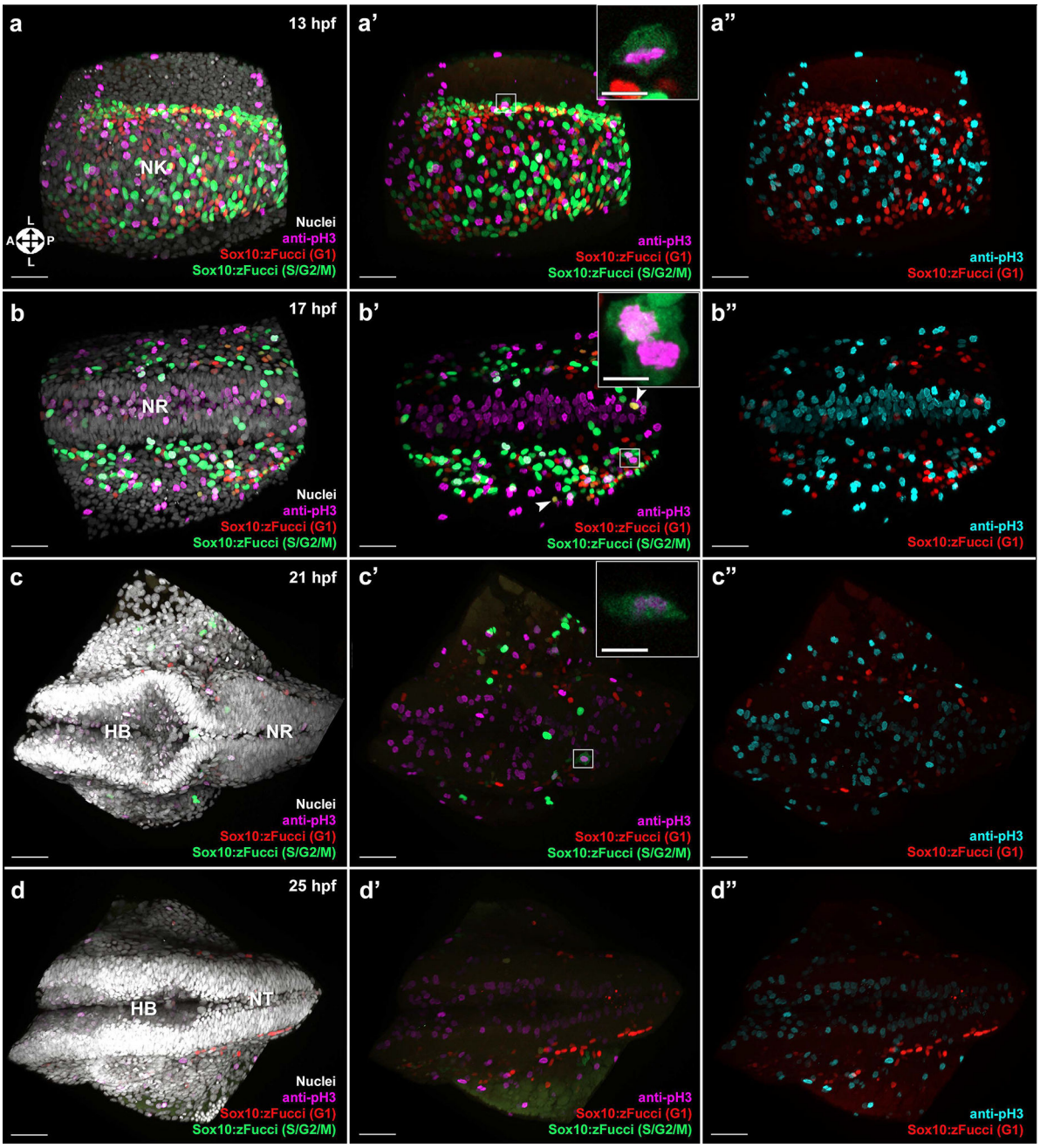

Figure 2. Sox10:zFucci accurately marks cell cycle progression

3D projections of anterodorsal views of Sox10:zFucci-positive embryos after whole mount immunofluorescence staining against pH3 (G2/M phase-specific) at 13 (a–a"), 17 (b–b"), 21 (c–c"), and 25 (d–d") hours post-fertilization (hpf). Insets (a',b',c') show 1 μm thick optical slices of Sox10:zFucci (S/G2/M); anti-pH3-dual positive cells. (Inset in (c') is slightly tilted from the 3D projection for clarity.) Arrowheads (b') indicate Sox10:zFucci (G1); Sox10:zFucci (S/G2/M)-dual positive cells. (a",b",c",d") 3D projections of Sox10:zFucci (G1) and anti-pH3 (teal) at each time point demonstrate that none of the observed Sox10:zFucci (G1)-positive cells are positive for pH3. NK: neural keel; NR: neural rod; NT:

neural tube; HB: hindbrain. All nuclei: white; anti-pH3: magenta/teal; Sox10:zFucci (G1): red nuclei; Sox10:zFucci (S/G2/M): green nuclei. Orientation arrows: A: anterior; P: posterior; L: lateral. Scale bars: 50 μm; insets: 12.5 μm.

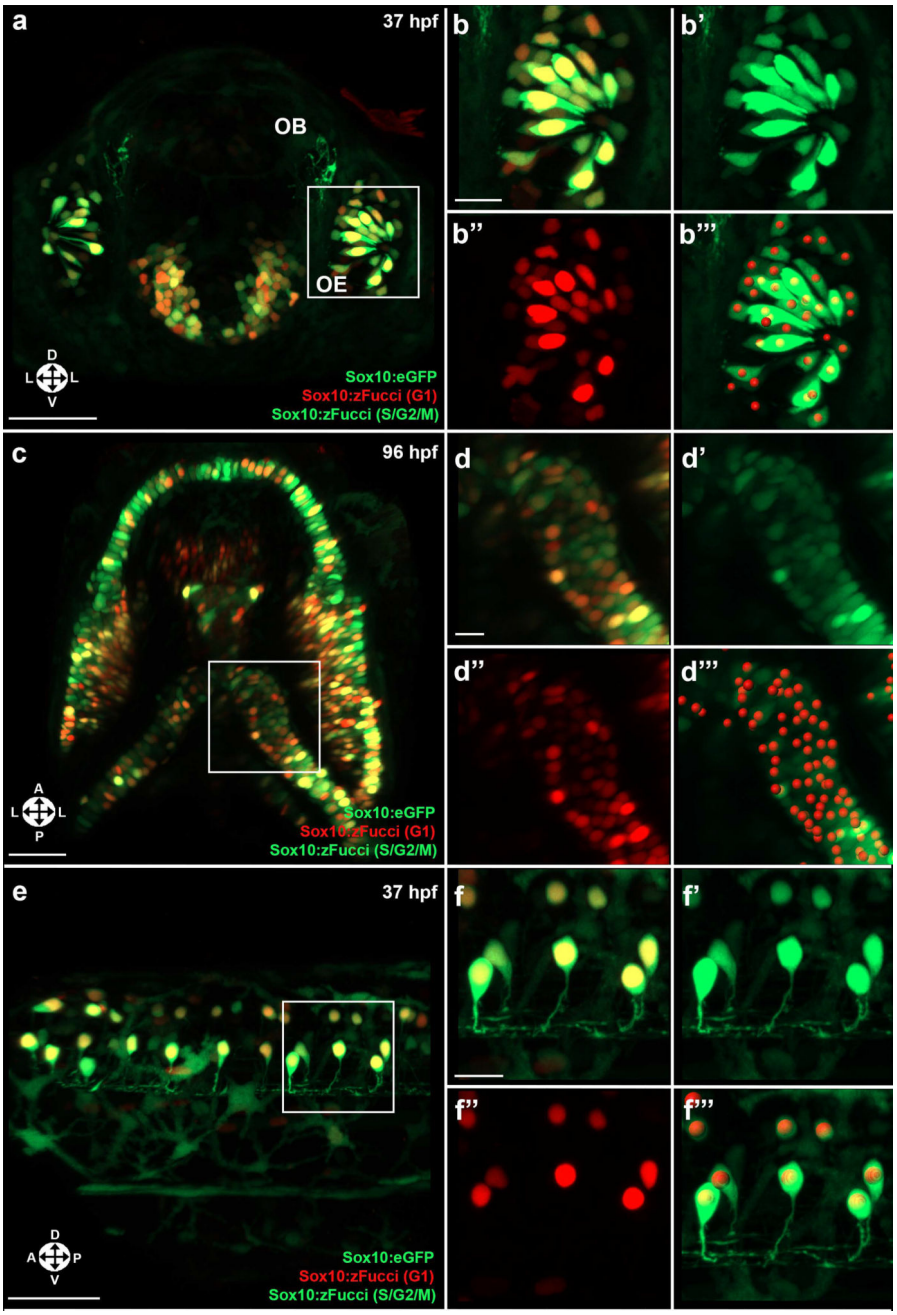

Figure 3. Sox10:zFucci and Sox10:eGFP overlap in neural crest-derived tissues

3D projections of cranial neural crest-derived tissues (a–d”’) and trunk neural crest-derived cells (e–f”’) in Sox10:zFucci; Sox10:eGFP-dual positive embryos. (a–b”’) At 37 hours post-fertilization (hpf), microvillous neurons in the olfactory epithelium (OE) are Sox10:zFucci; Sox10:eGFP-dual positive. (b–b”’) are magnified versions of the region marked by the white box in (a). (c–d”’) At 96 hpf, cartilage cells in the jaw are Sox10:zFucci; Sox10:eGFP-dual positive. (d–d”’) are magnified versions of the region marked by the white box in (c). (e–f”’) At 37 hpf, dorsal root ganglion neurons are Sox10:zFucci; Sox10:eGFP-dual positive. (f–f”’) are magnified versions of the region marked by the white box in (e). (b”’,d”’,f”’)

Imaris's 'Spots Analysis' was used to map out the overlap between Sox10:zFucci (G1)- (red spots) and Sox10:eGFP-positive cells. OB: olfactory bulb; OE: olfactory epithelium. Sox10:eGFP: green; Sox10:zFucci (G1): red nuclei; Sox10:zFucci (S/G2/M): green nuclei. Orientation arrows: A: anterior; P: posterior; D: dorsal; V: ventral; L: lateral. Scale bars: (a,c,e): 50 μm; (b–b"',d–d"',f–f"'): 12.5 μm.

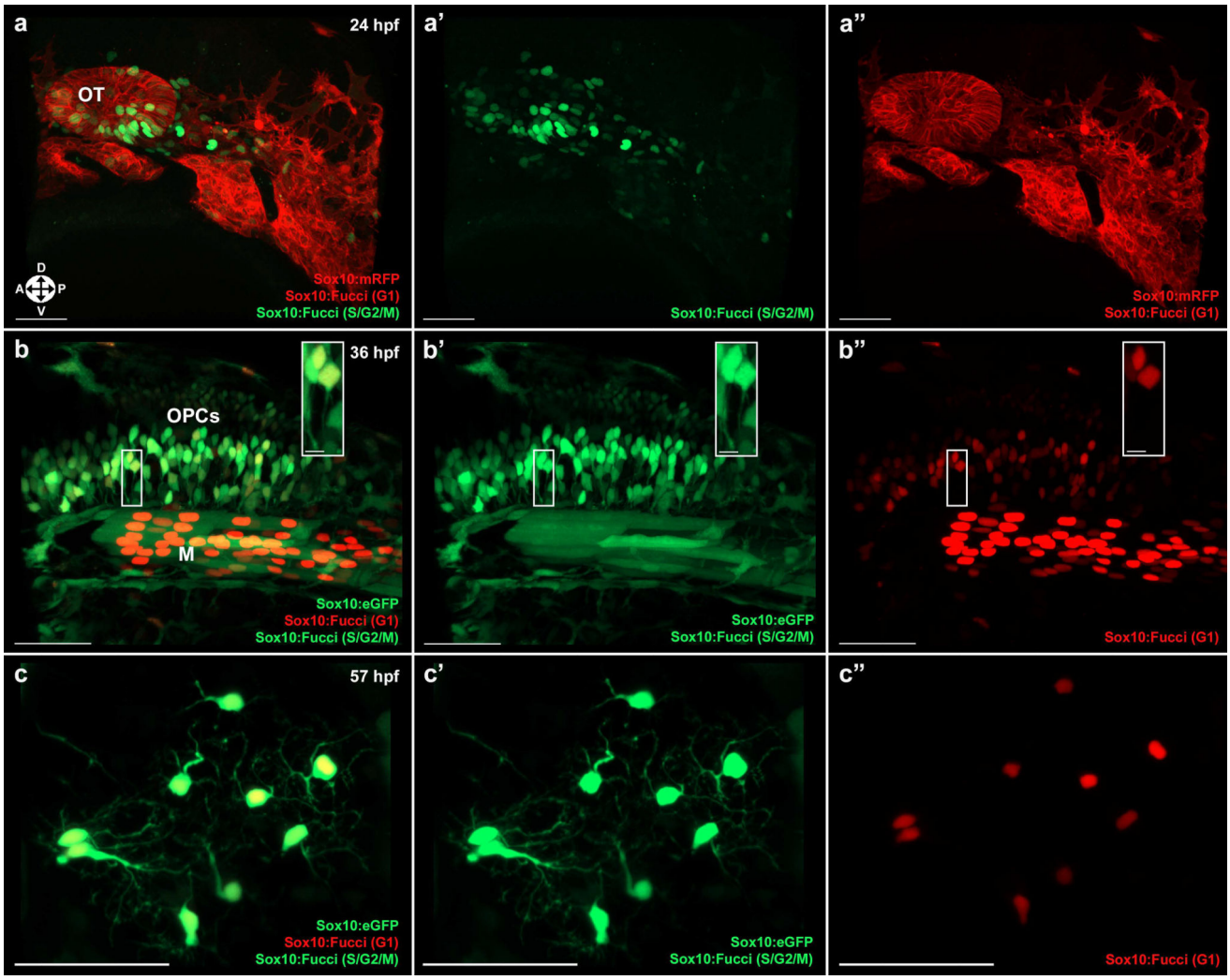

Figure 4. Sox10:zFucci marks several non-neural crest-derived tissues

3D projections of lateral views of Sox10:zFucci; Sox10:mRFP (a–a") and Sox10:zFucci; Sox10:eGFP (b–b")-dual positive embryos at 24 and 36 hours post-fertilization (hpf), respectively. (a–a") At 24 hpf, a subset of otic epithelial cells are Sox10:zFucci (S/G2/M); Sox10:mRFP-dual positive. (b–b") At 36 hpf, oligodendrocyte progenitor cells (OPCs) are Sox10:zFucci; Sox10:eGFP-dual positive. Insets (b–b") show OPCs dual positive for Sox10:zFucci and Sox10:eGFP. (c–c") Optical slices (2 μm thick) of OPCs at 57 hpf that are Sox10:zFucci; Sox10:eGFP-dual positive. OT: otic epithelium; OPCs: oligodendrocyte progenitor cells; M: muscle cells. Sox10:mRFP: red membranes; Sox10:eGFP: green; Sox10:zFucci (G1): red nuclei; Sox10:zFucci (S/G2/M): green nuclei. Orientation arrows: A: anterior; P: posterior; D: dorsal; V: ventral. Scale bars: 50 μm; insets: 12.5 μm.